Journal of Alzheimer's Disease 29 (2012) 1–4
IOS Press

Supplementary Data

Genomic and Nongenomic Signaling Induced by 1α,25(OH)$_2$-Vitamin D$_3$ Promotes the Recovery of Amyloid-β Phagocytosis by Alzheimer's Disease Macrophages

Mathew T. Mizwicki[a,*], Danusa Menegaz[a], Jun Zhang[b], Antonio Barrientos-Durán[a], Stephen Tse[c], John R. Cashman[d], Patrick R. Griffin[b] and Milan Fiala[c,*]
[a]*Department of Biochemistry, University of California, Riverside, CA, USA*
[b]*Department of Molecular Therapeutics, The Scripps Research Institute, Scripps Florida, Jupiter, FL, USA*
[c]*Department of Medicine, David Geffen School of Medicine at UCLA and VA Greater Los Angeles Healthcare System, Los Angeles, CA, USA*
[d]*Human BioMolecular Research Institute, San Diego, CA, USA*

Handling Associate Editor: Selma Yilmazer

Accepted 10 November 2011

*Correspondence to: Mathew T. Mizwicki (E-mail: mtmizwicki @gmail.com.) or Milan Fiala, UCLA CHS, 650 Charles E. Young Drive South, Room 23-338, Los Angeles, CA 90095-3517, USA. E-mail: fiala@mednet.ucla.edu.

ISSN 1387-2877/12/$27.50

Supplementary Table 1
Summary of the VDR-AP/GP/A-ring domain flexible docking results

Compound	Molecular Volume (cm^3)	Average LibDock Score		Average cDOCKER Interaction Energy (kcal/mole)	
	—	VDR-GP	VDR-AP	VDR-GP	VDR-AP
1,25D3	351.00	114	121	−70.8	−61.7
MK	339.30	124	112	−66.6	−57.6
CM#	263.62	94.7	100	−51.6	−52.2
BDC#	222.79	90.1	108	−50.7	−56.4
C180	320.28	77.8	88.8	−60.0	−57.1
DIDS	262.25	83.2	92.4*	−40.1	−39.2
U0126	253.70	72.7	84.2	−45.3	−47.3
Y27632	198.50	79.2	87.7	−38.6	−42.5
Calphostin c	491.47	No poses	No poses	No poses	No poses
IP_3(1,4,5)	194.75	95.0		−121	
IP_4(3,4,5,6)	224.18	101		−137	

The table summarizes the VDR flexible docking results obtained for 1,25D3, MK, CM, BDC, C180, DIDS, U1026, Y27632 and calphostin c when docked to 10 $Å^3$ VDR-AP/GP site spheres using the Discovery Studio 2.0 flexible docking module. The average LibDock scores and cDOCKER interaction energies (kcal/mole) for the top 7 complexes from each docking simulation are provided in the table. Supplementary Figures 3 and 4 provide snap shots of how these small molecules can bind to the VDR-AP and VDR-GP. For the inositolphosphates (IP_3 and IP_4), they did not form complexes with the VDR when they were docked in the VDR-AP/GP site spheres; however, when docked in the A-ring domain site sphere, stable IP-VDR complexes were observed (Fig. 5B and Supplementary Fig. 2) based on the LibDock and cDOCKER scores. The more positive the LibDock score and the more negative the cDOCKER interaction energy, the better the theoretical complex. An entry of 'no poses' in the table indicates that the ligand did not interact favorably with the VDR when the putative ligand was docked in the VDR-AP, VDR-GP or A-ring domain site spheres. The (*) indicates that DIDS was observed to occupy mostly the VDR-GP even when it was docked in the VDR-AP site sphere (see Supplementary Fig. 4C).

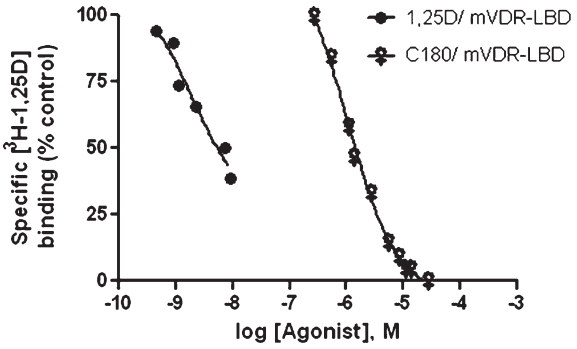

Supplementary Figure 1. 1,25D3 and C180 VDR (aa118-427, Δ165-215) affinity. The figure shows a representative competition curve used to measure the VDR K_i for 1,25D3 and C180. Briefly, 0.04 pmoles of [^{3}H]-1,25D3 was added to each tube and the ability of the given concentration of cold 1,25D3 or C180 to compete with the radiolabeled VDR ligand was measured by scintillation. K_i values were calculated using Prism 3.0. The average K_i for 1,25D3 is 3.2 nM ($n = 7$) and 2.2 μM for the curcumin synthetic analogue, C180 (Fig. 1).

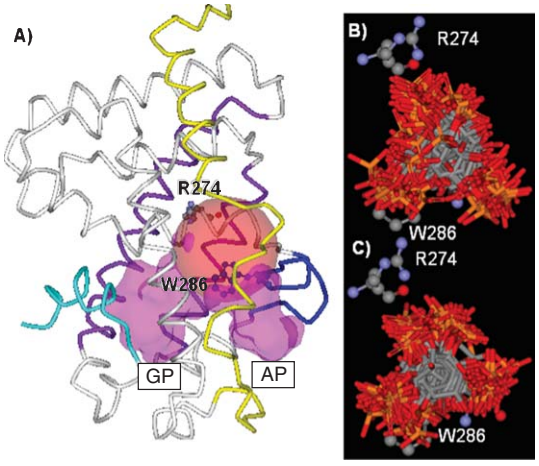

Supplementary Figure 2. Important VDR surfaces and the VDR A-ring domain and its putative natural ligands (i.e., inositolphosphates). A) A ribbon diagram of the VDR (aa120-427, Δ165-215). Colored ribbons highlight the hinge domain (yellow, aa118-164 in figure), consisting of helix-1 (H1, aa125-143), H2 (aa149-153) and random loop residues; a three stranded β-sheet (royal blue, aa279-295); H7/H10 (purple, aa306-323 and aa378-386); and H12 (cyan, aa415-423). H7/H10 form the region of the VDR associated with high affinity heterodimerization with the nuclear transcription factor, RXR. H12 (cyan) forms the bottom portion of the nuclear coactivator surface. The transparent purple region highlights the internal surface of the VDR available that is sampled by ligands. The overlapping A-ring domain is highlighted by the red transparent sphere. This is the site sphere used in docking inositolphosphates to the VDR (Table 1). B, C) The two panels show the overlay of the top 7 cDOCKER scored complexes for inositol 1,4,5-triphosphate (IP_3) and inositol3,4,5,6-tetraphosphate (IP_4), respectively. As in supplemental figures 3 and 4, R274 and W286 are labeled and rendered ball and stick to help orient the reader.

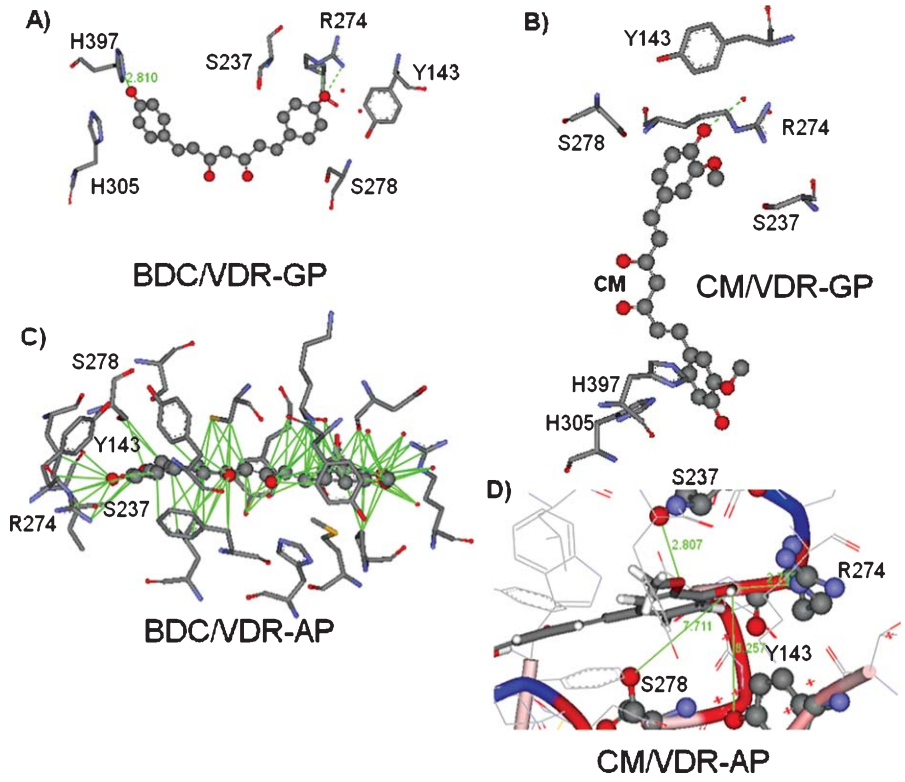

Supplementary Figure 3. The highest affinity VDR-GP and VDR-AP CM and BDC flexible docking complexes. A, B) Show representative models obtained when CM or BDC was flexibly docked to the VDR-GP. H-bonds formed between the curcuminoid and VDR-GP residues are indicated by solid lines and the distance in $\mathring{A}$ listed. C, D) Depict representative models obtained when CM or BDC was flexibly docked to the VDR-AP. H-bonds formed between the curcuminoid and VDR-AP residues are indicated by solid lines and the distance in $\mathring{A}$ listed (D). In C, all contacts made between the ligand and VDR-AP within 4.0 $\mathring{A}$ are indicated by solid green lines. In A-D, the A-ring domain residues, Y143, S237, R274, and S278 are labeled.

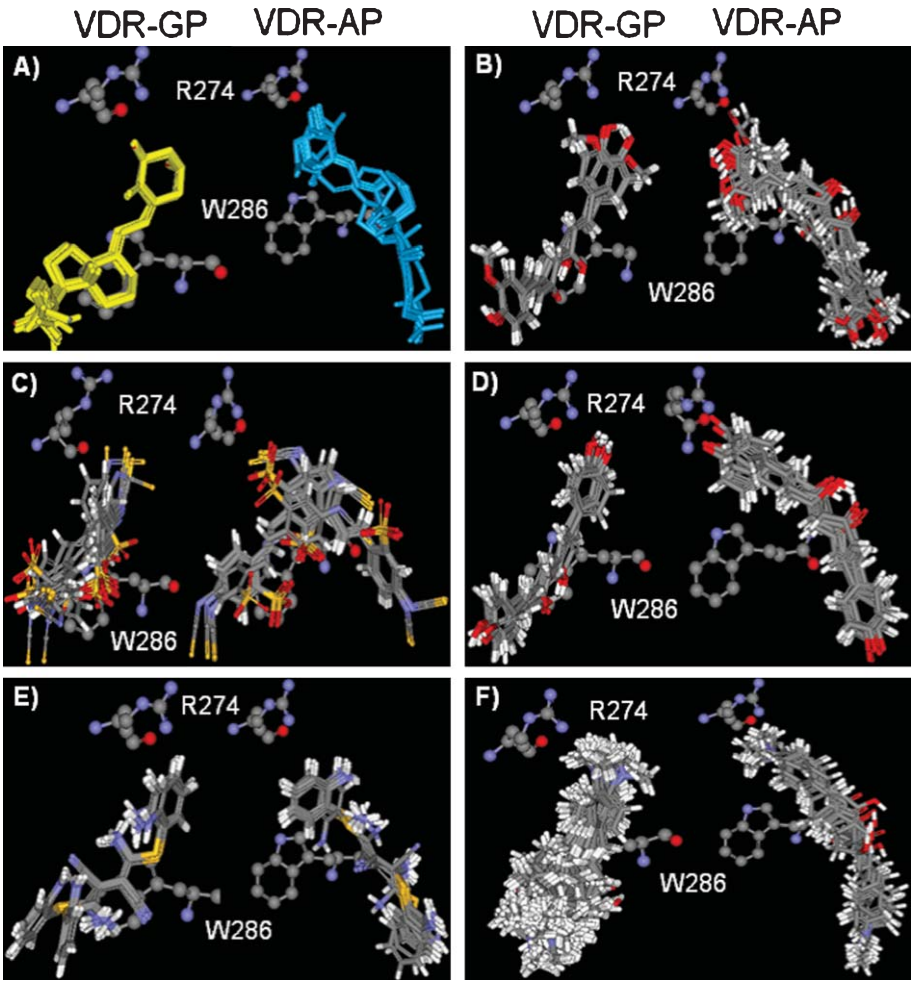

Supplementary Fig. 4. Ligand dynamics observed in the VDR-GP or VDR-AP. A-F depict the heterogeneity observed for each VDR ligand (A: 1,25D3; B: curcumin; C: DIDS; D: BDC; E: U0126; and F: C180, see Fig. 1 for chemical structures) when docked to the VDR-GP or VDR-AP (Fig. 5A and Supplementary Fig. 2). In each panel, the top 7 cDOCKER scored complexes (i.e., ligand poses) of the given ligand are overlaid. For 1,25D3 the structures of the different poses are colored yellow and light blue to distinguish the VDR-GP from the VDR-AP. In each panel the R274 and W286 residues are rendered in ball and stick and can be used to discern the relative positioning of the ligands with respect to one another. Briefly, 1,25D3, CM, BDC and C180 all form electrostatic and/or vdW contacts with R274 when docked in the VDR-GP or VDR-AP. Alternatively, U0126 (E) does not form any stabilizing contact with R274 in either the VDR-GP or VDR-AP. DIDS (C) is unique in that it preferred to bind to the VDR-GP, even when first placed in the VDR-AP to begin the flexible docking simulation. This is just one example of how each ligand is both similar to and/or different when compared to the dynamic molecular contacts made by 1,25D3 when docked in either pocket.